The EMBO Journal Vol. 20 No. 15 pp. 3902–3909, 2001

Mycobacterium tuberculosis hemoglobin N displays a protein tunnel suited for O_2 diffusion to the heme

Mario Milani[1,2], Alessandra Pesce[1], Yannick Ouellet[3], Paolo Ascenzi[1,4], Michel Guertin[3] and Martino Bolognesi[1,5]

[1]Department of Physics-INFM and Advanced Biotechnology Center-IST, University of Genova, Largo Rosanna Benzi 10. 16132 Genova, [2]Istituto Giannina Gaslini, Largo Gerolamo Gaslini 5. 16147 Genova, [4]Department of Biology, University 'Roma Tre', Viale Guglielmo Marconi 446. 00146 Roma, Italy and [3]Departement de Biochimie et de Microbiologie, Pavillon Marchand, Université Laval, Faculté des Sciences et de Génie, Quebec G1K 7P4, Canada

[5]Corresponding author
e-mail: bolognes@fisica.unige.it

Macrophage-generated oxygen- and nitrogen-reactive species control the development of *Mycobacterium tuberculosis* infection in the host. *Mycobacterium tuberculosis* 'truncated hemoglobin' N (trHbN) has been related to nitric oxide (NO) detoxification, in response to macrophage nitrosative stress, during the bacterium latent infection stage. The three-dimensional structure of oxygenated trHbN, solved at 1.9 Å resolution, displays the two-over-two α-helical sandwich fold recently characterized in two homologous truncated hemoglobins, featuring an extra N-terminal α-helix and homodimeric assembly. In the absence of a polar distal E7 residue, the O_2 heme ligand is stabilized by two hydrogen bonds to TyrB10(33). Strikingly, ligand diffusion to the heme in trHbN may occur via an apolar tunnel/cavity system extending for ~28 Å through the protein matrix, connecting the heme distal cavity to two distinct protein surface sites. This unique structural feature appears to be conserved in several homologous truncated hemoglobins. It is proposed that in trHbN, heme Fe/O_2 stereochemistry and the protein matrix tunnel may promote O_2/NO chemistry *in vivo*, as a *M.tuberculosis* defense mechanism against macrophage nitrosative stress.

Keywords: hemoprotein structure/macrophage oxidative stress/*Mycobacterium tuberculosis*/nitric oxide/truncated hemoglobins

Introduction

Current epidemiological statistics indicate that about one-third of the human population is latently infected with *Mycobacterium tuberculosis*. It is estimated that 23% of the infected people eventually display the full infection. Moreover, 80% of those who are infected live in developing countries, where the infection is lethal in half of the cases (see http://www.nature.com/nm/special_focus/tb/). In most healthy individuals, the initial *M.tuberculosis* infection is contained by the immune system, which forces the bacteria to enter a latent state for several years with possible reactivation later in life. The initial event after infection involves multiplication of *M.tuberculosis* inside the host macrophage. Later, infected macrophages are isolated from the circulation by newly recruited macrophages to form the so-called caseous granuloma (Bloom, 1994), whose (bio)chemical environment restricts growth of the bacteria (Cunningham and Spreadbury, 1998).

Several independent lines of evidence indicate that macrophage-generated oxygen- and nitrogen-reactive species can restrict the development of *M.tuberculosis* infection in the host (MacMicking *et al*., 1997; Manca *et al*., 1999). Interestingly, nitric oxide (NO) and related reactive species are produced by inducible NO-synthase in the macrophages during the initial infection stage, and may be involved in restricting the bacteria during the latent stage (MacMicking *et al*., 1997). In turn, *M.tuberculosis* has evolved defense mechanisms against oxygen- and nitrogen-reactive species. Specifically, reactive oxygen species may be scavenged by a catalase-peroxidase system encoded by the *katG* gene (Heym *et al*., 1993; Manca *et al*., 1999; Flynn and Chan, 2001). Moreover, the *M.tuberculosis* alkyl hydroperoxide reductase is capable of reaction with peroxynitrite *in vitro*, based on a reactive Cys pair, thereby suggesting a detoxifying role *in vivo* (Bryk *et al*., 2000). On the other hand, Couture *et al*. (1999a) argued that the protection of bacilli against nitrogen-reactive species during latency in the granuloma relies on the oxygenated derivative of a homodimeric 'truncated hemoglobin' (trHbN), encoded by the *glbN* gene. All of the above macromolecular systems are potential targets for the development of new anti-tuberculosis drugs.

Truncated hemoglobins (trHbs) are small heme proteins (Couture *et al*., 1999a,b, 2000; Thorsteinsson *et al*., 1999; Das *et al*., 2000; Pesce *et al*., 2000) widely distributed in bacteria, unicellular eukaryotes and higher plants, forming a distinct group within the hemoglobin (Hb) superfamily (Moens *et al*., 1996). When compared with vertebrate and nonvertebrate Hbs, trHbs display sequence identity <15%. Crystallographic studies of trHbs from the green unicellular alga *Chlamydomonas eugametos* and the ciliated protozoan *Paramecium caudatum* (C-trHb and P-trHb, respectively) have shown that trHb tertiary structure is based on a two-over-two α-helical sandwich (Pesce *et al*., 2000), rather than on the three-over-three α-helical sandwich of the classical Hb fold (Perutz, 1979). The heme-linked proximal HisF8 residue is the only residue conserved throughout the Hb and trHb families; in trHbs, the CD1 residue is mostly Phe, being occasionally substituted by Leu or Tyr. The main heme-ligand stabilizing residue in the distal pocket is invariantly TyrB10, with only two known exceptions (Figure 1) (Pesce *et al*., 2000).

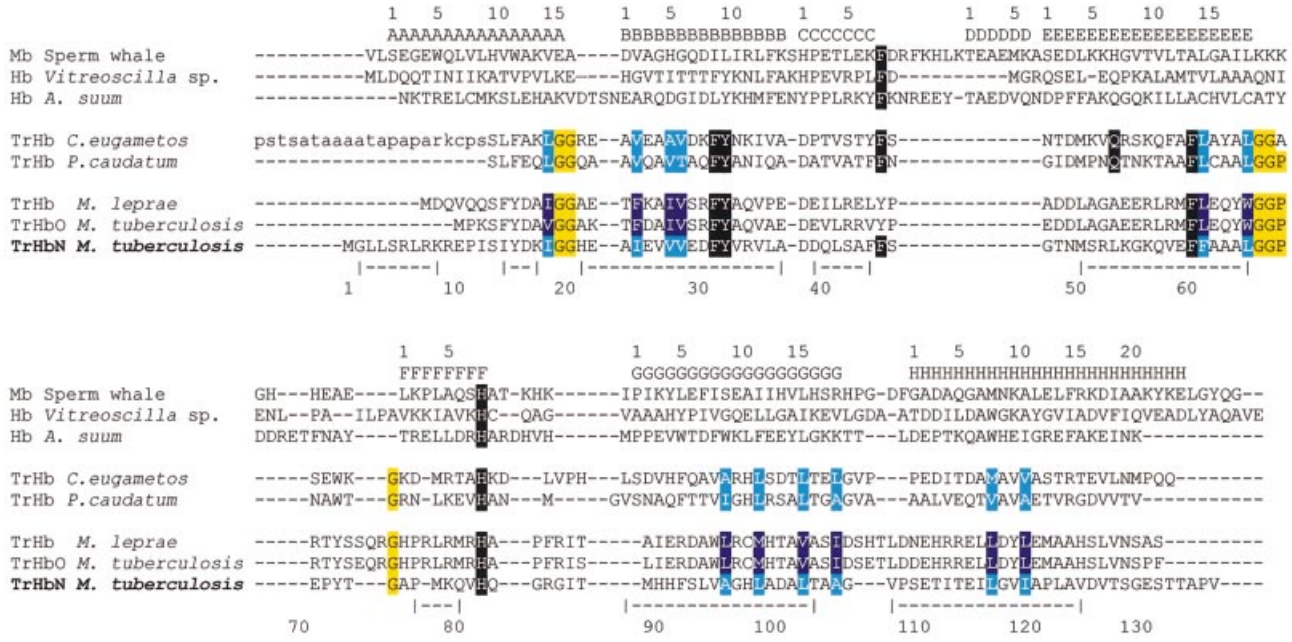

Fig. 1. Structure-based amino acid sequence alignment of selected trHbs, relative to sperm whale Mb, *Vitreoscilla sp.* Hb and *Ascaris suum* Hb. Topological sites referred to the classical globin fold are indicated on top of the alignments; amino acid sequence numbering as well as α-helical regions (indicated by |- - -| segments) refer to trHbN. Black boxes highlight key residues conserved in trHbs, and PheCD1 and HisF8 residues in conventional Hbs/Mbs. Gly-based motifs in trHbs are boxed in yellow. The conserved residues lining the apolar protein tunnel in trHbN, C-trHb and P-trHb are highlighted in cyan, while the corresponding residues held to build the apolar tunnel in *Mycobacterium leprae* trHb and *M.tuberculosis* trHbO are highlighted in blue. TrHbO is a second trHb found in *M.tuberculosis* (18% amino acid sequence identity to trHbN). Moreover, the sequence identity of trHbN with C-trHb and P-trHb is 39 and 37%, respectively.

In vivo, the high oxygen affinity of trHbN (P_{50} ~0.01 mm Hg) may ensure a low but critical level of oxygen, granting survival of *M.tuberculosis* in the granuloma hypoxic environment when the bacilli enter latency (Couture *et al*., 1999a). It has been proposed that the oxygenated trHbN (oxy-trHbN) could detoxify from macrophage-generated NO, similarly to the dioxygenase activity of (flavo)Hbs and myoglobin (Mb), which convert NO to nitrate (Gardner *et al*., 1998; Liu *et al*., 2000; Poole and Hughes, 2000; Brunori, 2001a; Flögel *et al*., 2001; Frauenfelder *et al*., 2001). Interestingly, resonance Raman spectra of O_2, CO and OH^- ligated forms suggest that the trHbN heme Fe coordination may be suited for performing O_2/NO chemistry (Yeh *et al*., 2000).

Here we report the crystal structure of wild-type oxy-trHbN, the third known protein structure within the trHb family, at 1.9 Å resolution (*R* factor: 19.0%). We show that the homodimeric trHbN is characterized by an unprecedented N-terminal α-helix and by an extended protein cavity/tunnel system, which may be a conserved route for ligand diffusion to/from the heme in trHbs.

Results and discussion

The two-over-two α-helical fold of trHbN

In keeping with the conservation of specific-sequence motifs (Figure 1), trHbN displays the recently characterized trHb fold, mainly based on the B, E, G and H α-helices of the classical globin fold (Figure 2A) (Pesce *et al*., 2000). The two oxy-trHbN chains present in the crystallographic asymmetric unit display very similar structures [root mean square deviation (r.m.s.d.) of 0.7 Å for 127 C_α atom pairs]. Despite considerable divergence at the amino acid sequence level (see Figure 1), structural superpositions of oxy-trHbN (chain A) on C-trHb and on P-trHb yield r.m.s.d. values of 1.1 and 1.0 Å, respectively (for 106 C_α atom pairs). Comparison with the bacterial *Vitreoscilla sp.* Hb (Tarricone *et al*., 1997) and sperm whale Mb (Kachalova *et al*., 1999) indicates that in the two proteins only 44 and 54 C_α pairs can be matched to trHbN, with r.m.s.d. values of 2.6 and 2.1 Å, respectively. Such a limited number of matched C_α pairs is indicative of the extensive structural deviations, particularly localized on the heme proximal side, distinguishing the trHb fold from the conventional globin fold (Pesce *et al*., 2000).

A comparative analysis of the main structural features characterizing the trHb family (Figures 1 and 2A) shows clear structural conservation of the main protein regions held to be crucial for stabilization of the trHb fold. Among these are a one-turn A-helix, tying the N-terminal region to the protein core, the short (3_{10}) C-helix, supporting PheCD1(46), and the E-helix, hosting residue LeuE7(54) and the trHb-invariant PheE14(61). A ten-residue extended polypeptide segment (identified as pre-F) on the heme proximal side is followed by a one-turn helix (F-helix), supporting the heme-iron coordinating residue HisF8(81). Moreover, as noted from the analysis of available trHb amino acid sequences (Pesce *et al*., 2000) (Figure 1), three conserved Gly-based motifs, located at the AB, E–pre-F and pre-F–F secondary structure transition regions, are crucial for the achievement of the trHbN fold.

Heme stabilization in trHbN is provided by both propionates, through hydrogen bonds to ThrCD4(49) and Ala(75), and also via salt bridges to ArgE6(53) and

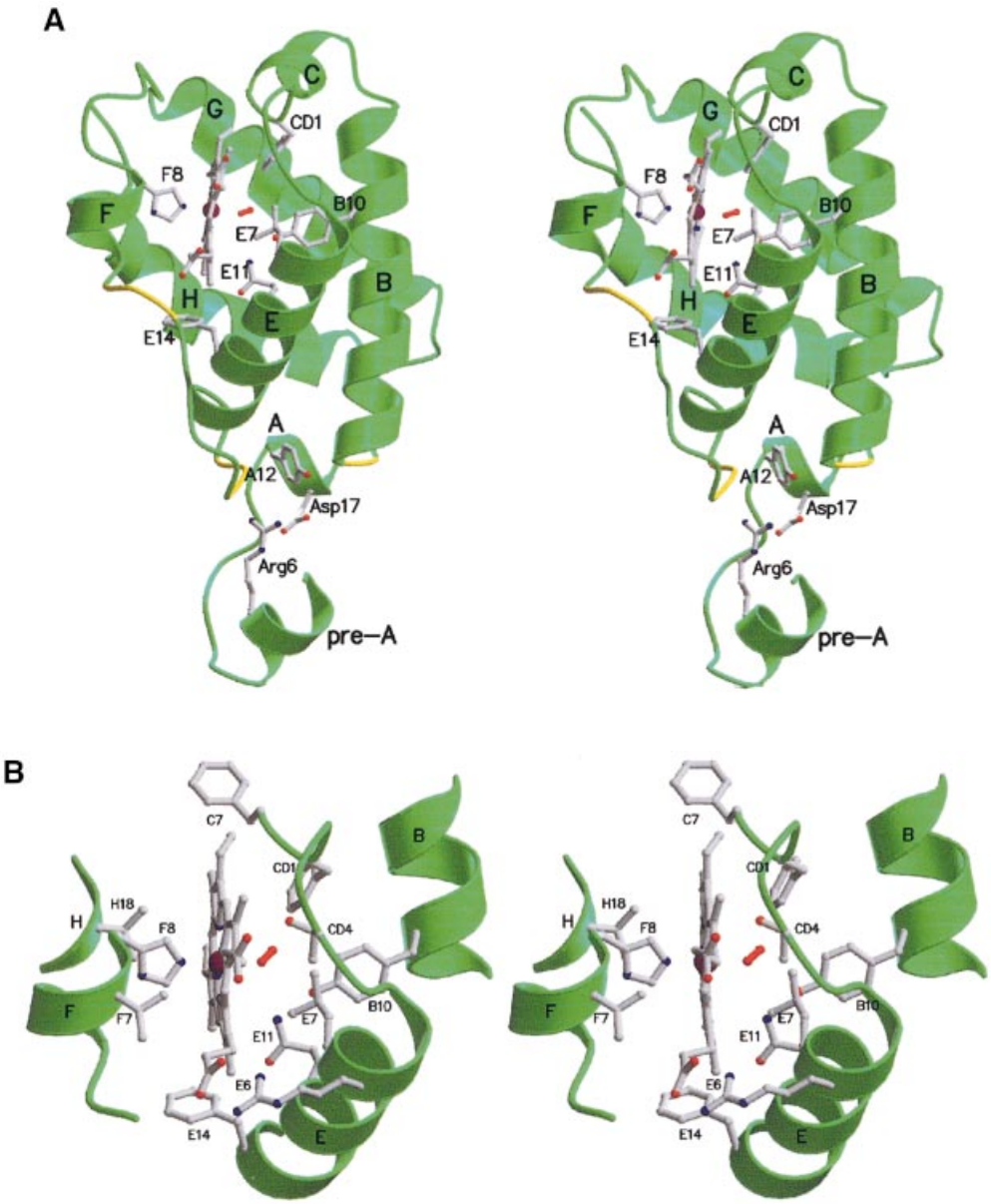

Fig. 2. (**A**) Ribbon stereo view of trHbN (A-chain), including the heme group, the O_2 molecule (red) and some of the residues deemed relevant for trHb fold stability or for trHbN functionality. Locations of the invariant Gly-based motifs are highlighted in yellow. Secondary structure elements are labeled in black. All figures were drawn with MOLSCRIPT (Kraulis, 1991) and Raster3D (Merritt and Bacon, 1997). (**B**) A stereo view of the main distal and proximal site residues in trHbN, together with the O_2 molecule (in red), the heme group, the one-turn F-helix and segments of helices B, E and H.

ArgFG3(84). Several residues prevent exposure of the heme to solvent. Among these, the trHb invariant PheE14(61) residue falls almost orthogonal to the porphyrin ring, next to the CHD methinic bridge (Figure 2A). Together with residue Tyr(72) (from the pre-F loop), PheE14(61) is held to provide an efficient closure of the lower part of the heme pocket. Similarly, hydrogen-bonded side chains connecting residues of the E-helix and residues of the pre-F region completely hinder solvent accessibility to the heme distal site. These interactions, together with 51 van der Waals contacts (<4.0 Å), may be crucial not only for stabilization of the trHbN bound heme, but also for defining the conformation of the extended pre-F loop.

In a context showing a general conservation of the trHb fold, two novel structural features distinguishing trHbN from the homologous C-trHb and P-trHb are the presence of additional secondary structure at the trHbN N-terminus, and its homodimeric assembly. The 12-residue insertion observed at the trHbN N-terminus (Figures 1 and 2) builds a short pre-A α-helix [Gly(2)–Lys(9)] and an extended tetrapeptide [Arg(10)–Ile(13)], protruding from the compact protein fold. A highly polar sequence motif (Arg-Leu-Arg-Lys-Arg, in the 6–10 pre-A region) may be responsible for the breakdown of the elongated α-helix expected here for a conventionally folded Hb. Moreover, an intramolecular hydrogen-bonded salt bridge between residues Arg(6) and AspA13(17), and crystal packing

Table I. Stereochemistry of trHbN heme Fe coordination

	Chain-A	Chain-B
Average Fe–N(pyrrole) (Å)	1.99	1.98
HisF8 NE2–Fe (Å)	2.10	2.11
Fe–O (ligand) (Å)	2.19	2.07
Fe-heme plane deviation (Å)[a]	0.014	–0.028
Fe–O-O (°)	113	109
Tilt angle (°)[b]	1.7	1.5
Dihedral NA-Fe–NE2-CE1 (°)	29	39

[a]Positive values indicate Fe atom displacement out of the porphyrin plane towards the distal site; negative values indicate displacements towards the proximal site.
[b]Angle between the proximal HisF8 NE2–Fe bond and the heme normal.

contacts to the G-helix and the pre-F loop, may support the orientation of the pre-A segment. Remarkably, N-terminal α-helical structures reminiscent of the trHbN pre-A region have been observed in the Hb fold resembling phycocyanin (Schirmer *et al*., 1985), whereas an extended polypeptide segment and a short α-helix preceding the fully extended A-helix are present in the classical globin fold of sea lamprey Hb (Heaslet and Royer, 1999) and *Scapharca* Hb (Condon and Royer, 1994), respectively. No evident structural relation links the trHbN pre-A region to these proteins.

Gel filtration analysis of the recombinant protein suggested that trHbN has a dimeric assembly (Couture *et al*., 1999a). Accordingly, a dimer based on direct intermolecular contacts provided by the C-helix, FG loop and H-helix of each trHbN subunit can be recognized within the molecular packing of the orthorhombic crystal form examined. The dimer has an elongated shape, positioning the two hemes 22 Å apart, and is endowed with quasi-two-fold symmetry. The interface area between the two trHbN chains is, however, limited, being ~310 Å^2. Such putative quaternary assembly, essentially based on van der Waals contacts and five water-mediated hydrogen bonds, has no counterpart in known Hbs (Bolognesi *et al*., 1997).

Heme proximal and distal sites in oxy-trHbN

Residue MetF4(77) starts the one-turn F-helix, being in contact with the heme A pyrrole ring and the methinic CHA bridge. The carbonyl group of MetF4(77) is hydrogen bonded to the side chain of HisF8(81), whose azimuthal orientation with respect to the porphyrin ring is dictated by this interaction and by contacts to the side chains of ValF7(80) and ValH18(126) (Figure 2B). Hydrogen bonding of the heme proximal imidazole ring to the carbonyl group of Met(44)F4 is a structural feature frequently observed in Hbs from different phyla (Bolognesi *et al*., 1997). HisF8(81) imidazole is staggered with respect to the pyrrole N atoms (Table I), being fully solvent inaccessible due to the shielding action of residues MetF4(77), ValF7(80), ValH18(126) and ArgFG3(84). The HisF8(81)–Fe coordination bond is 2.11 and 2.10 Å, in trHbN subunits A and B, respectively, while the Fe atom is essentially contained within the heme pyrrole N-atoms plane (Table I). The staggered azimuthal orientation of HisF8(81) imidazole is indicative of an unstrained proximal His, as expected from the high value (226 cm^{-1}) of the resonance Raman Fe–His bond stretching frequency (Couture *et al*., 1999a; Yeh *et al*., 2000). Moreover, the staggered HisF8(81) orientation favours the in-plane position of the Fe atom, possibly supporting fast O_2 association (k_{on} = 25 μM^{-1}s^{-1} in trHbN) and specific activation of the heme distal ligand, as suggested for the heme Fe role in peroxidases (Dawson, 1988; Yeh *et al*., 2000; Mukai *et al*., 2001).

The dioxygen ligand in trHbN is fully buried within the distal site cavity. In fact, due to the orientation of the E helix close to the heme distal side, and to the location of the side chains of ThrCD4(49), ArgE6(53), LeuE7(54) and LysE10(57), solvent access to the distal site cavity through the classical E7-gate path is completely impaired (Figure 2B) (Bolognesi *et al*., 1982; Perutz, 1989; Scott *et al*., 2001). In both subunits the O_2 molecule is tilted by ~110° relative to the Fe axial bond, and is oriented towards the rear end of the heme crevice, pointing in the direction of residue ValG8(94). Thus, both oxygen atoms in the O_2 molecule are at hydrogen-bonding distance from the phenolic OH group of TyrB10(33) (average value, 3.12 Å). Notably, resonance Raman investigations on oxy-trHbN have recently suggested that stabilization of the heme-bound O_2 occurs through a hydrogen bond between the TyrB10(33) OH group and the proximal O atom of the ligand (Yeh *et al*., 2000). Moreover, site-specific mutation of TyrB10(33) into either Leu or Phe results in a 100-fold increase in the O_2 dissociation rate constant, and in a shift of the Fe–O_2 bond stretching frequency from 560 to 570 cm^{-1}, i.e. to a stretching frequency identical to that of vertebrate and nonvertebrate oxygenated Hbs and Mbs (Couture *et al*., 1999a; Yeh *et al*., 2000). In agreement with the establishment of hydrogen bonds between the heme-bound dioxygen and the distal TyrB10(33) residue, the O_2 dissociation rate constant for trHbN is low (k_{off} = 0.199 s^{-1}), comparable to those of C-trHb, *Cyanobacterium synechocystis* trHb and *Ascaris* Hb bearing the distal TyrB10-GlnE7 residue pair. However, it should be noted that the TyrB10-GlnE7 pair in different Hbs is not always a prerequisite leading to strong stabilization of the heme-bound O_2 (Travaglini-Allocatelli *et al*., 1994; Couture *et al*., 1999b, 2000; Das *et al*., 2000, 2001).

The distal LeuE7(54) residue is >4 Å away from the O_2 molecule, whereas the GlnE11(58) NE2 atom is at 3.8 Å from both ligand O atoms, in both trHbN subunits. In agreement with these structural observations, resonance Raman spectra are indicative of the absence of hydrogen bonding between O_2 and GlnE11(58) (Yeh *et al*., 2000). However, in the crystal structure, GlnE11(58) NE2 atom is hydrogen bonded to the OH atom of TyrB10(33) (2.83 and 3.12 Å, in subunits A and B, respectively). Next, the heme-bound dioxygen distal O atom falls at 4 Å from the rim of the aromatic ring of PheCD1(46), in both subunits.

A ligand diffusion tunnel through trHbN

The most striking structural feature characterizing trHbN is the presence of an almost continuous tunnel through the protein matrix, connecting the heme distal pocket to the protein surface at two distinct sites. One access to the tunnel is located between the AB and GH hinge regions (Figure 3A). The second tunnel access is defined by the G- and H-helix residues AlaG9(95), LeuG12(98) and

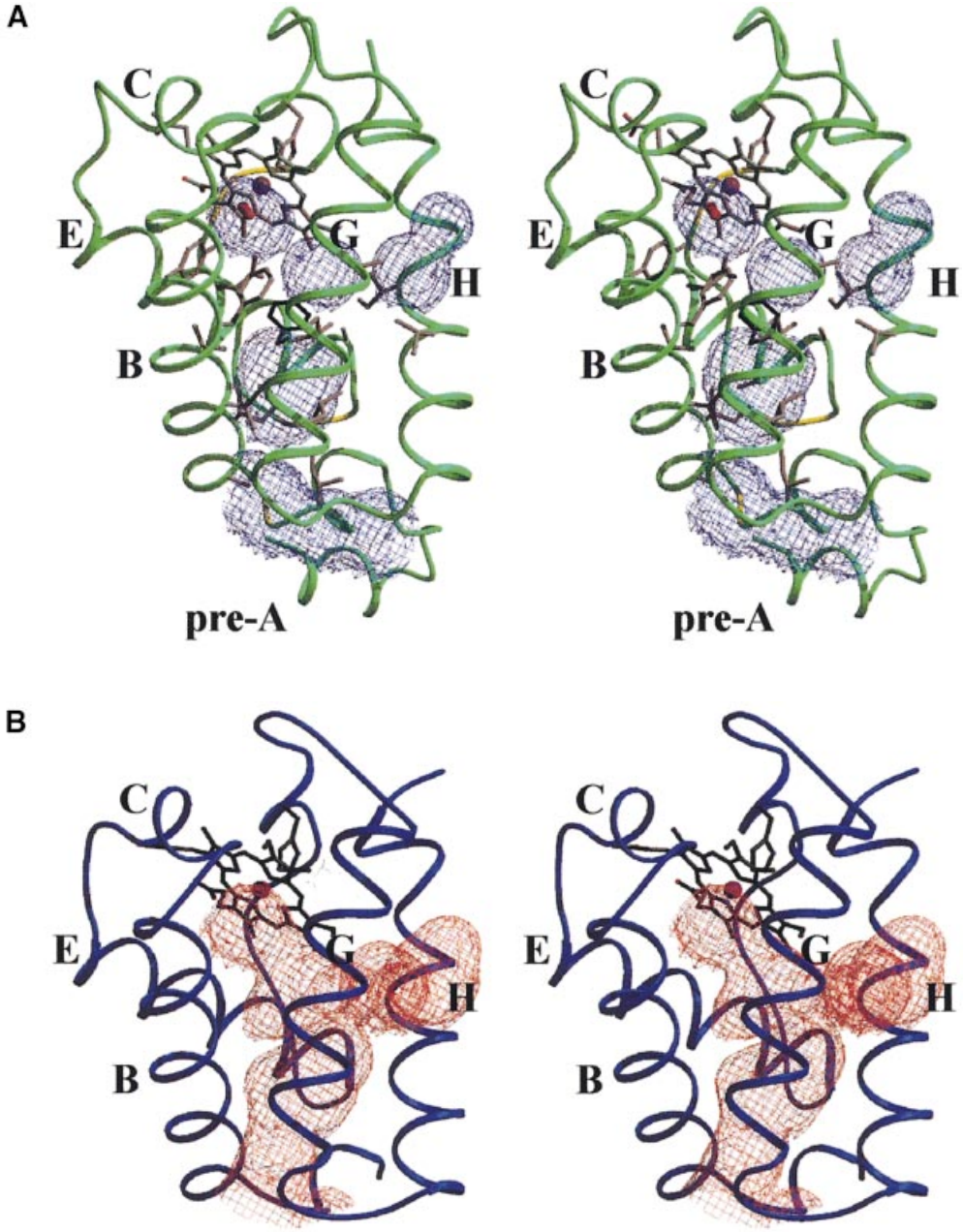

Fig. 3. (**A**) Stereo view of the protein matrix tunnel observed in trHbN. The tunnel surface, defined by a 1.4 Å radius probe, is portrayed in light blue. The distal site cavity surface is calculated and displayed in the absence of the O_2 molecule, which is, however, shown in red for reference. Residue PheE15(62), causing the main restriction to the tunnel diameter, is shown in black; the other residues lining the tunnel walls are portrayed in gray. The estimated tunnel volume is ~330 $Å^3$. (**B**) For comparison, C-trHb protein backbone (blue) is portrayed in the same orientation as in Figure 3A, together with the protein matrix tunnel surface (orange), calculated as described above. Capital letters identify selected α-helices in the trHb fold. Both trHbs are shown approximately in the same orientation and scale.

IleH11(119), next to the distal face of the heme B-pyrrole ring (Figure 3A). The tunnel can be seen as being composed of two orthogonal branches, stretching ~20 and 8 Å from the respective access sites to the heme ligand site. The tunnel has a diameter of 5 to 7 Å, with one restriction [~4 Å at the mutually facing residues PheE15(62) and LeuG12(98)]. The residues defining both tunnel access sites and lining its inner surface are all of apolar nature [IleA15(19), AlaB1(24), IleB2(25), ValB5(28), ValB6(29), PheB9(32), PheE15(62), AlaE16(63), LeuE19(66), LeuG12(98), LeuG16(102) and AlaG19(105) on the main tunnel branch; AlaG9(95), LeuH8(116) and IleH11(119) on the short tunnel branch].

The heme-bound O_2 falls at the intersection of the two tunnel branches, where the distal residues TyrB10(33) and GlnE11(58) are located. Moreover, residue PheE15(62) restricting the main tunnel stretch is observed in two alternate conformations (differing by 63° by rotation around the C_α–C_β bond) in subunit A. Considering that heme distal site access via the E7-gate is prevented by clustering of distal side chains, the trHbN tunnel may provide an efficient diffusion path for O_2 and other small

ligands (e.g. NO), achieving an O_2 association rate constant (k_{on} = 25 $M^{-1}s^{-1}$; Couture *et al*., 1999a) comparable to that of sperm whale Mb and other conventional Hbs or Mbs endowed with the HisE7 gating residue. In this respect, the PheE15(62) alternate conformations observed in trHbN may reflect a gating role played by this residue in modulating ligand diffusion to/from the heme iron atom, along the longer tunnel branch.

It is worth noticing that, although only marginally considered before, both C-trHb and P-trHb display tunnel/cavity features at comparable locations within the trHb fold (Pesce *et al*., 2000). Figure 3B shows that in the chloroplast C-trHb the topological location of such tunnel/cavity system closely matches that of trHbN, with deviations reflecting local structural variability in the two proteins. For example, in view of the PheE15(62)→LeuE15(49) substitution, in C-trHb, no tunnel restriction site is present in the main tunnel branch. Similar conclusions can be drawn for P-trHb.

Further to the above discussion, inspection of the available trHb amino acid sequences indicates that residues lining the identified tunnel region are hydrophobic and strongly conserved throughout the family (Figure 1). The above observations suggest that trHbs may be endowed with a conserved tunnel/cavity system, facilitating ligand diffusion from the protein surface to the heme. Remarkably, vertebrate and nonvertebrate Hbs, which can support ligand access to the heme distal site through the E7-gate (Perutz, 1989; Scott *et al*., 2001), never display such an extended and accessible tunnel/cavity system through the protein matrix, which appears a unique feature of the trHb family. Nevertheless, smaller isolated cavities in sperm whale Mb have been deemed important for ligand (re)binding, hopping, escape trajectory to the solvent, and promotion of bimolecular reactions, thus being central for the proposed role of Mb as a pseudo-enzyme (Brunori, 2000, 2001a,b; Flögel *et al*., 2001; Frauenfelder *et al*., 2001; Scott *et al*., 2001).

Conclusions

Very recently it has been suggested that trHbN may be involved in O_2-sustained NO detoxification (Couture *et al*., 1999a), similarly to what has been proposed for (flavo)Hbs and Mb (Gardner *et al*., 1998; Liu *et al*., 2000; Poole and Hughes, 2000; Brunori, 2001a; Flögel *et al*., 2001; Frauenfelder *et al*., 2001). On the other hand, NO-activated O_2 detoxification has been reported for *Ascaris* Hb (Minning *et al*., 1999). The results reported here indicate that the protein tunnel observed in trHbN has the structural properties required for O_2 and NO diffusion through the protein matrix. Moreover, the observed unstrained heme Fe proximal coordination, O_2 binding stereochemistry and TyrB10(33) hydrogen bonding may effectively support polarization and orientation of the reactants, which would promote O_2/NO chemistry (Yeh *et al*., 2000; Das *et al*., 2001). Indeed, preliminary results show that titration of oxy-trHbN with NO *in vitro* results in immediate stoichiometric oxidation of the protein, with subsequent formation of the NO-met form (M.Guertin, unpublished data).

TrHbN three-dimensional structure supports a general principle of protein evolution, whereby modulation of the active site structure within homologous proteins may result in widely different substrate specificities. In the case of the Hb and trHb families, the role played by the distal TyrB10 residue is paradigmatic in showing a shift from a ligand stabilization role (in O_2 storage/transport in vertebrate Hbs) to a proposed catalytic role in a dioxygenase reaction (for trHbN; Couture *et al*., 1999a). We notice that evolution of such different functionalities has required, in trHbs, extensive remodeling of the globin fold well outside of the active site region, likely resulting in an entirely new O_2 diffusion path within the protein matrix, towards the (catalytic) heme distal site. The observed properties of trHbs in prokaryotic pathogens, for which intracellular O_2 diffusion would not be a limiting factor to metabolism, further suggest that *in vivo*, trHbs may bind (and activate) dioxygen for cellular roles other than O_2 transport.

Table II. Data collection and refinement statistics

Data collection statistics	
Wavelength (Å)	0.931
Resolution (Å)	40–1.9
Mosaicity (°)	0.86
Completeness (%)	95.1 (88.9)[a]
R_{merge} (%)	5.3 (33.1)
Independent reflections	20772
Average $I/\sigma(I)$	13 (3)
Redundancy	3.5 (2.3)
Refinement statistics and model quality	
Resolution range (Å)	40–1.9
Total no. of non-hydrogen atoms	1890
No. of water molecules	233
R factor/R_{free} (%)[b]	19.0/24.3
Space group	$P2_12_12_1$
Unit cell (Å)	a = 44.8, b = 62.2, c = 91.0
R.m.s.d. from ideal geometry	
bond lengths (Å)	0.012
bond angles (°)	1.4
Ramachandran plot[c]	
most favoured region	97.7%
additional allowed region	2.3%
Averaged B factors (Å^2)	
main chain	28
side chain	34
solvent	40

[a]Outer shell statistics (1.93–1.90 Å) within parentheses.
[b]Calculated using 5% of the reflections.
[c]Data produced with the program PROCHECK (Laskowski *et al*., 1993).

Materials and methods

Recombinant wild-type oxy-trHbN was cloned, expressed and purified to homogeneity as described elsewhere (Couture *et al*., 1999a). Oxy-trHbN (23 mg/ml protein concentration) was crystallized by micro-dialysis against a reservoir containing 1.8 M K_2HPO_4/KH_2PO_4 pH 8.3 at 4°C. Diffraction data were collected from one crystal [soaked for 20 s in a cryo-protectant solution containing 20% (v/v) glycerol, 1.9 M K_2HPO_4/KH_2PO_4 pH 8.2, before flash-freezing at 100 K] at ESRF (Grenoble, France; beam line ID14–3), indexed/processed with the DENZO and CCP4 programs (CCP4, 1994; Otwinowski and Minor, 1997). Oxy-trHbN crystals belong to the orthorhombic space group $P2_12_12_1$, with unit cell constants a = 44.80 Å, b = 62.25 Å, c = 91.02 Å, two molecules per asymmetric unit. A first molecular replacement solution was searched using a trimmed model of C-trHb and structure factors previously measured on a cyano-met trHbN crystal [using the program AMoRe

(Navaza and Saludjian, 1997); data in the 15–3.5 Å resolution range yielded a correlation coefficient of 54.2% and an *R* factor of 45.8%, after both molecules in the asymmetric unit were located; our unpublished results]. Crystallographic refinement of the search model against oxy-trHbN data and manual rebuilding (Jones *et al*., 1991) allowed us to complete the two molecules (program CNS with bulk solvent correction; Brünger *et al*., 1998). The refined oxy-trHbN model contains residues 2–128 for subunit A, and residues 2–127 for subunit B (1890 protein atoms), two dioxygen ligands, 233 water molecules and three phosphate ions (*R* factor = 19.0%, R_{free} factor = 24.3%, at 1.9 Å resolution). Data collection and refinement statistics are shown in Table II. Atomic coordinates and structure factors for oxy-trHbN have been deposited with the Protein Data Bank (accession code: 1idr; Berman *et al*., 2000).

Analysis of the trHbN tunnel/cavity system has been carried out using the SURFNET program (Laskowski, 1995).

Acknowledgements

This work was supported by grants from the Italian Space Agency (IR/167/01), the Ministry of University and Scientific Research of Italy (Structural Genomics Project), and the CNR Target Project Biotecnologie, to M.B. and P.A., and by the National Sciences and Engineering Research Council of Canada, Grant 06P0046306, to M.G. M.B. is grateful to Institute 'G. Gaslini' for continuous support.

References

Berman,H.M., Westbrook,J., Feng,Z., Gilliland,G., Bhat,T.N., Weissig,H., Shindyalov,I.N. and Bourne,P.E. (2000) The Protein Data Bank. *Nucleic Acids Res.*, **28**, 235–242.

Bloom,B.R. (ed.) (1994) *Tuberculosis: Pathogenesis*, *Protection and Control.* ASM Press, Washington, DC.

Bolognesi,M., Cannillo,E., Ascenzi,P., Giacometti,G.M., Merli,A. and Brunori,M. (1982) Reactivity of ferric *Aplysia* and sperm whale myoglobins towards imidazole. X-ray and binding study. *J. Mol. Biol.*, **158**, 305–315.

Bolognesi,M., Bordo,D., Rizzi,M., Tarricone,C. and Ascenzi,P. (1997) Nonvertebrate hemoglobins: structural bases for reactivity. *Prog. Biophys. Mol. Biol.*, **68**, 29–68.

Brünger,A.T. *et al.* (1998) Crystallography and NMR System: a new software suite for macromolecular structure determination. *Acta Crystallogr. D*, **54**, 905–921.

Brunori,M. (2000) Structural dynamics of myoglobin. *Biophys. Chem.*, **86**, 221–230.

Brunori,M. (2001a) Nitric oxide, cytochrome-*c* oxidase and myoglobin. *Trends Biochem. Sci.*, **26**, 21–23.

Brunori,M. (2001b) Nitric oxide moves myoglobin centre stage. *Trends Biochem. Sci.*, **26**, 209–210.

Bryk,R., Griffin,P. and Nathan,C. (2000) Peroxynitrite reductase activity of bacterial peroxiredoxins. *Nature*, **407**, 211–215.

CCP4 (1994) The CCP4 Suite: programs for protein crystallography. *Acta Crystallogr. D*, **50**, 760–763.

Condon,P.J. and Royer,W.E. (1994) Crystal structure of oxygenated *Scapharca* dimeric hemoglobin at 1.7 Å resolution. *J. Biol. Chem.*, **269**, 25259–25267.

Couture,M., Yeh,S., Wittenberg,B.A., Wittenberg,J.B., Ouellet,Y., Rousseau,D.L. and Guertin,M. (1999a) A cooperative oxygen-binding hemoglobin from *Mycobacterium tuberculosis*. *Proc. Natl Acad. Sci. USA*, **96**, 11223–11228.

Couture,M., Das,T.K., Lee,H.C., Peisach,J., Rousseau,D.L., Wittenberg, B.A., Wittenberg,J.B. and Guertin,M. (1999b) *Chlamydomonas* chloroplast ferrous hemoglobin. Heme pocket structure and reactions with ligands. *J. Biol. Chem.*, **274**, 6898–6910.

Couture,M., Das,T.K., Savard,P.Y., Ouellet,Y., Wittenberg,J.B., Wittenberg,B.A., Rousseau,D.L. and Guertin,M. (2000) Structural investigations of the hemoglobin of the *Cyanobacterium synechocystis* PCC6803 reveal a unique distal heme pocket. *Eur. J. Biochem.*, **267**, 4770–4780.

Cunningham,A.F. and Spreadbury,C.L. (1998) Mycobacterial stationary phase induced by low oxygen tension: cell wall thickening and localization of the 16-kilodalton alpha-crystallin homolog. *J. Bacteriol.*, **180**, 801–808.

Das,T.K., Weber,R.E., Dewilde,S., Wittenberg,J.B., Wittenberg,B.A., Yamauchi,K., Van Hauwaert,M.L., Moens,L. and Rousseau,D.L. (2000) Ligand binding in the ferric and ferrous states of *Paramecium* hemoglobin. *Biochemistry*, **39**, 14330–14340.

Das,T.K., Couture,M., Ouellet,Y., Guertin,M. and Rousseau,D.L. (2001) Simultaneous observation of the O–O and Fe–O_2 stretching modes in oxyhemoglobins. *Proc. Natl Acad. Sci. USA*, **98**, 479–484.

Dawson,J.H. (1988) Probing structure–function relations in heme-containing oxygenases and peroxidases. *Science*, **240**, 433–439.

Flögel,U., Merx,M.W., Gödecke,A., Decking,U.K. and Schrader,J. (2001) Myoglobin: a scavenger of bioactive NO. *Proc. Natl Acad. Sci. USA*, **98**, 735–740.

Flynn,J.L. and Chan,J. (2001) Immunology of tuberculosis. *Annu. Rev. Immunol.*, **19**, 93–129.

Frauenfelder,H., McMahan,B.H., Austin,R.H., Chu,K. and Groves,J.T. (2001) The role of structure, energy landscape, dynamics and allostery in the enzymatic function of myoglobin. *Proc. Natl Acad. Sci. USA*, **98**, 2370–2374.

Gardner,P.R., Gardner,A.M., Martin,L.A. and Salzman,A.L. (1998) Nitric oxide dioxygenase: an enzymic function for flavohemoglobin. *Proc. Natl Acad. Sci. USA*, **95**, 10378–10383.

Heaslet,H.A. and Royer,W.E. (1999) The 2.7 Å crystal structure of deoxygenated hemoglobin from the sea lamprey (*Petromyzon marinus*): structural basis for a lowered oxygen affinity and Bohr effect. *Structure*, **7**, 517–526.

Heym,B., Zhang,Y., Poulet,S., Young,D. and Cole,S.T. (1993) Characterization of the *katG* gene encoding a catalase-peroxidase required for the isoniazid susceptibility of *Mycobacterium tuberculosis*. *J. Bacteriol*., **175**, 4255–4259.

Jones,T.A., Zou,J.Y., Cowan,S.W. and Kjeldgaard,M. (1991) Improved methods for building protein models in electron density maps and the location of errors in these models. *Acta Crystallogr. A*, **47**, 110–119.

Kachalova,G.S., Popov,A.N. and Bartunik,H.D. (1999) A steric mechanism for inhibition of CO binding to heme proteins. *Science*, **284**, 473–476.

Kraulis,P.J. (1991) MOLSCRIPT: a program to produce both detailed and schematic plots of protein structures. *J. Appl. Crystallogr.*, **24**, 946–950.

Laskowski,R.A., MacArthur,M.W., Moss,D.S. and Thornton,J.M. (1993) PROCHECK, a program to check the stereochemical quality of protein structures. *J. Appl. Crystallogr.*, **26**, 283–291.

Laskowski,R.A. (1995) SURFNET: a program for visualizing molecular surfaces, cavities and intermolecular interactions. *J. Mol. Graph.*, **13**, 323–330.

Liu,L., Zeng,M., Hausladen,A., Heitman,J. and Stamler,J.S. (2000) Protection from nitrosative stress by yeast flavohemoglobin. *Proc. Natl Acad. Sci. USA*, **97**, 4672–4676.

MacMicking,J.D., North,R.J., LaCourse,R., Mudgett,J.S., Shah,S.K. and Nathan,C.F. (1997) Identification of nitric oxide synthase as a protective locus against tuberculosis. *Proc. Natl Acad. Sci. USA*, **94**, 5243–5248.

Manca,C., Paul,S., Barry,C.E.,III, Freedman,V.H. and Kaplan,G. (1999) *Mycobacterium tuberculosis* catalase and peroxidase activities and resistance to oxidative killing in human monocytes *in vitro*. *Infect. Immun.*, **67**, 74–79.

Merritt,E.A. and Bacon,D.J. (1997) Raster3D: photorealistic molecular graphics. *Methods Enzymol.*, **277**, 505–524.

Minning,D.M., Gow,A.J., Bonaventura,J., Braun,R., Dewhirst,M., Goldberg,D.E. and Stamler,J.S. (1999) *Ascaris* haemoglobin is a nitric oxide-activated 'deoxygenase'. *Nature*, **401**, 497–502.

Moens,L., Vanfleteren,J., Van de Peer,Y., Peeters,K., Kapp,O., Czeluzniak,J., Goodman,M., Blaxter,M. and Vinogradov,S. (1996) Globins in nonvertebrate species: dispersal by horizontal gene transfer and evolution of the structure–function relationship. *Mol. Biol. Evol.*, **13**, 324–333.

Mukai,M., Mills,C.E., Poole,R.K. and Yeh,S. (2001) Flavohemoglobin: a globin with a peroxidase-like catalytic site. *J. Biol. Chem.*, **276**, 7272–7277.

Navaza,J. and Saludjian,P. (1997) AMoRe: an automated molecular replacement program package. *Methods Enzymol.*, **276**, 581–594.

Otwinowski,Z. and Minor,W. (1997) Processing of X-ray diffraction data collected in oscillation mode. *Methods Enzymol.*, **276**, 307–326.

Perutz,M.F. (1979) Regulation of oxygen affinity of hemoglobin: influence of structure of the globin on the heme iron. *Annu. Rev. Biochem.*, **48**, 327–386.

Perutz,M.F. (1989) Myoglobin and haemoglobin: role of distal residues in reactions with haem ligands. *Trends Biochem. Sci.*, **14**, 42–44.

Pesce,A., Couture,M., Dewilde,S., Guertin,M., Yamauchi,K., Ascenzi,P., Moens,L. and Bolognesi,M. (2000) A novel two-over-two α-helical

sandwich fold is characteristic of the truncated hemoglobin family. *EMBO J.*, **19**, 2424–2434.

Poole,R.K. and Hughes,M.N. (2000) New functions for the ancient globin family: bacterial responses to nitric oxide and nitrosative stress. *Mol. Microbiol.*, **36**, 775–783.

Schirmer,T., Bode,W., Huber,R., Sidler,W. and Zuber,H. (1985) X-ray crystallographic structure of the light-harvesting biliprotein C-phycocyanin from the thermophilic cyanobacterium *Mastigocladus laminosus* and its resemblance to globin structures. *J. Mol. Biol.*, **184**, 257–277.

Scott,E.E., Gibson,Q.H. and Olson,J.S. (2001) Mapping the pathways for O_2 entry into and exit from myoglobin. *J. Biol. Chem.*, **276**, 5177–5188.

Tarricone,C., Galizzi,A., Coda,A., Ascenzi,P. and Bolognesi,M. (1997) Unusual structure of the oxygen-binding site in the dimeric bacterial hemoglobin from *Vitreoscilla sp. Structure*, **5**, 497–507.

Thorsteinsson,M.V., Bevan,D.R., Potts,M., Dou,Y., Eich,R.F., Hargrove, M.S., Gibson,Q.H. and Olson,J.S. (1999) A cyanobacterial hemoglobin with unusual ligand binding kinetics and stability properties. *Biochemistry*, **38**, 2117–2126.

Travaglini-Allocatelli,C., Cutruzzola,F., Brancaccio,A., Vallone,B. and Brunori,M. (1994) Engineering *Ascaris* hemoglobin oxygen affinity in sperm whale myoglobin: role of tyrosine B10. *FEBS Lett.*, **352**, 63–66.

Yeh,S., Couture,M., Ouellet,Y., Guertin,M. and Rousseau,D.L. (2000) A cooperative oxygen binding hemoglobin from *Mycobacterium tuberculosis*. Stabilization of heme ligands by a distal tyrosine residue. *J. Biol. Chem.*, **275**, 1679–1684.

Received April 23, 2001; revised June 15, 2001; accepted June 19, 2001